Conditional Density Estimation with Dimensionality Reduction via Squared-Loss Conditional Entropy Minimization

Voot Tangkaratt
Ning Xie
Masashi Sugiyama
Tokyo Institute of Technology
voot@sg.cs.titech.ac.jp
xie@sg.cs.titech.ac.jp
sugi@cs.titech.ac.jp
http://sugiyama-www.cs.titech.ac.jp/~sugi

Abstract

Regression aims at estimating the conditional mean of output given input. However, regression is not informative enough if the conditional density is multimodal, heteroscedastic, and asymmetric. In such a case, estimating the conditional density itself is preferable, but conditional density estimation (CDE) is challenging in high-dimensional space. A naive approach to coping with high-dimensionality is to first perform dimensionality reduction (DR) and then execute CDE. However, such a two-step process does not perform well in practice because the error incurred in the first DR step can be magnified in the second CDE step. In this paper, we propose a novel single-shot procedure that performs CDE and DR simultaneously in an integrated way. Our key idea is to formulate DR as the problem of minimizing a squared-loss variant of conditional entropy, and this is solved via CDE. Thus, an additional CDE step is not needed after DR. We demonstrate the usefulness of the proposed method through extensive experiments on various datasets including humanoid robot transition and computer art.

Keywords

Conditional density estimation, dimensionality reduction.

1 Introduction

Analyzing input-output relationship from samples is one of the central challenges in machine learning. The most common approach is *regression*, which estimates the conditional mean of output $\boldsymbol{y}$ given input $\boldsymbol{x}$. However, just analyzing the conditional mean is not

informative enough, when the conditional density $p(\boldsymbol{y}|\boldsymbol{x})$ possesses multimodality, asymmetry, and heteroscedasticity (i.e., input-dependent variance) as a function of output $\boldsymbol{y}$. In such cases, it would be more appropriate to estimate the conditional density itself (Figure 2).

The most naive approach to conditional density estimation (CDE) would be *ϵ-neighbor kernel density estimation* (ϵ-KDE), which performs standard KDE along $\boldsymbol{y}$ only with nearby samples in the input domain. However, ϵ-KDE do not work well in high-dimensional problems because the number of nearby samples is too few. To avoid the small sample problem, KDE may be applied twice to estimate $p(\boldsymbol{x}, \boldsymbol{y})$ and $p(\boldsymbol{x})$ separately and the estimated densities may be plugged into the decomposed form $p(\boldsymbol{y}|\boldsymbol{x}) = p(\boldsymbol{x}, \boldsymbol{y})/p(\boldsymbol{x})$ to estimate the conditional density. However, taking the ratio of two estimated densities significantly magnifies the estimation error and thus is not reliable. To overcome this problem, an approach to directly estimating the density ratio $p(\boldsymbol{x}, \boldsymbol{y})/p(\boldsymbol{x})$ without separate estimation of densities $p(\boldsymbol{x}, \boldsymbol{y})$ and $p(\boldsymbol{x})$ has been explored (Sugiyama et al., 2010). This method, called *least-squares CDE* (LSCDE), was proved to possess the optimal non-parametric learning rate in the mini-max sense, and its solution can be efficiently and analytically computed. Nevertheless, estimating conditional densities in high-dimensional problems is still challenging.

A natural idea to cope with the high-dimensionality is to perform *dimensionality reduction* (DR) before CDE. *Sufficient DR* (Li, 1991; Cook and Ni, 2005) is a framework of supervised DR aimed at finding the subspace of input $\boldsymbol{x}$ that contains all information on output $\boldsymbol{y}$, and a method based on conditional-covariance operators in reproducing kernel Hilbert spaces has been proposed (Fukumizu et al., 2009). Although this method possesses superior theoretical properties, it is not easy to use in practice because no systematic model selection method is available for kernel parameters. To overcome this problem, an alternative sufficient DR method based on *squared-loss mutual information* (SMI) has been proposed recently (Suzuki and Sugiyama, 2013). This method involves non-parametric estimation of SMI that is theoretically guaranteed to achieve the optimal estimation rate, and all tuning parameters can be systematically chosen in practice by cross-validation with respect to the SMI approximation error.

Given such state-of-the-art DR methods, performing DR before LSCDE would be a promising approach to improving the accuracy of CDE in high-dimensional problems. However, such a two-step approach is not preferable because DR in the first step is performed without regard to CDE in the second step and thus small error incurred in the DR step can be significantly magnified in the CDE step.

In this paper, we propose a single-shot method that integrates DR and CDE. Our key idea is to formulate the sufficient DR problem in terms of the *squared-loss conditional entropy* (SCE) which includes the conditional density in its definition, and LSCDE is executed when DR is performed. Therefore, when DR is completed, the final conditional density estimator has already been obtained without an additional CDE step (Figure 1). We demonstrate the usefulness of the proposed method, named *least-squares conditional entropy* (LSCE), through experiments on benchmark datasets, humanoid robot control simulations, and computer art.

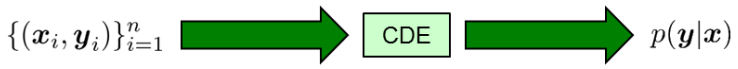

(a) CDE without DR

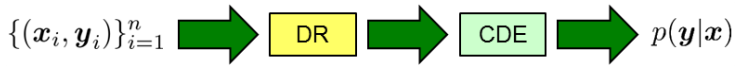

(b) CDE after DR

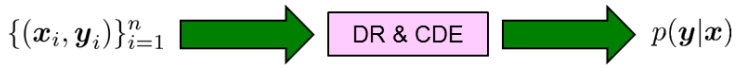

(c) CDE with DR (proposed)

Figure 1: Conditional density estimation (CDE) and dimensionality reduction (DR). (a) CDE without DR performs poorly in high-dimensional problems. (b) CDE after DR can magnify the small DR error in the CDE step. (c) CDE with DR (proposed) performs CDE in the DR process in an integrated manner.

2 Conditional Density Estimation with Dimensionality Reduction

In this section, we describe our proposed method for conditional density estimation with dimensionality reduction.

2.1 Problem Formulation

Let $\mathcal{D}_{\mathbf{x}}(\subset \mathbb{R}^{d_{\mathbf{x}}})$ and $\mathcal{D}_{\mathbf{y}}(\subset \mathbb{R}^{d_{\mathbf{y}}})$ be the input and output domains with dimensionality $d_{\mathbf{x}}$ and $d_{\mathbf{y}}$, respectively, and let $p(\boldsymbol{x}, \boldsymbol{y})$ be a joint probability density on $\mathcal{D}_{\mathbf{x}} \times \mathcal{D}_{\mathbf{y}}$. Assume that we are given n independent and identically distributed (i.i.d.) training samples from the joint density:

$$\{(\boldsymbol{x}_i, \boldsymbol{y}_i)\}_{i=1}^n \overset{\text{i.i.d.}}{\sim} p(\boldsymbol{x}, \boldsymbol{y}).$$

The goal is to estimate the conditional density $p(\boldsymbol{y}|\boldsymbol{x})$ from the samples.

Our implicit assumption is that the input dimensionality $d_{\mathbf{x}}$ is large, but its "intrinsic" dimensionality, denoted by $d_{\mathbf{z}}$, is rather small. More specifically, let $\boldsymbol{W}$ and $\boldsymbol{W}_\perp$ be $d_{\mathbf{z}} \times d_{\mathbf{x}}$ and $(d_{\mathbf{x}} - d_{\mathbf{z}}) \times d_{\mathbf{x}}$ matrices such that $\left[\boldsymbol{W}^\top, \boldsymbol{W}_\perp^\top\right]$ is an orthogonal matrix. Then we assume that $\boldsymbol{x}$ can be decomposed into the component $\boldsymbol{z} = \boldsymbol{W}\boldsymbol{x}$ and its perpendicular component $\boldsymbol{z}_\perp = \boldsymbol{W}_\perp \boldsymbol{x}$ so that $\boldsymbol{y}$ and $\boldsymbol{x}$ are conditionally independent given $\boldsymbol{z}$:

$$\boldsymbol{y} \perp\!\!\!\perp \boldsymbol{x} | \boldsymbol{z}. \tag{1}$$

This means that $\boldsymbol{z}$ is the relevant part of $\boldsymbol{x}$, and the rest $\boldsymbol{z}_\perp$ does not contain any information on $\boldsymbol{y}$. The problem of finding $\boldsymbol{W}$ is called *sufficient dimensionality reduction* (Li, 1991; Cook and Ni, 2005).

2.2 Sufficient Dimensionality Reduction with SCE

Let us consider a squared-loss variant of conditional entropy named *squared-loss CE* (SCE):

$$\mathrm{SCE}(\boldsymbol{Y}|\boldsymbol{Z}) = -\frac{1}{2}\iint \Big(p(\boldsymbol{y}|\boldsymbol{z}) - 1\Big)^2 p(\boldsymbol{z})\mathrm{d}\boldsymbol{z}\mathrm{d}\boldsymbol{y}. \tag{2}$$

By expanding the squared term in Eq.(2), we obtained

$$\begin{aligned}
\mathrm{SCE}(\boldsymbol{Y}|\boldsymbol{Z}) &= -\frac{1}{2}\iint p(\boldsymbol{y}|\boldsymbol{z})^2 p(\boldsymbol{z})\mathrm{d}\boldsymbol{z}\mathrm{d}\boldsymbol{y} + \iint p(\boldsymbol{y}|\boldsymbol{z})p(\boldsymbol{z})\mathrm{d}\boldsymbol{z}\mathrm{d}\boldsymbol{y} - \frac{1}{2}\iint p(\boldsymbol{z})\mathrm{d}\boldsymbol{z}\mathrm{d}\boldsymbol{y} \\
&= -\frac{1}{2}\iint p(\boldsymbol{y}|\boldsymbol{z})^2 p(\boldsymbol{z})\mathrm{d}\boldsymbol{z}\mathrm{d}\boldsymbol{y} + 1 - \frac{1}{2}\int \mathrm{d}\boldsymbol{y} \\
&= \widetilde{\mathrm{SCE}}(\boldsymbol{Y}|\boldsymbol{Z}) + 1 - \frac{1}{2}\int \mathrm{d}\boldsymbol{y},
\end{aligned} \tag{3}$$

where $\widetilde{\mathrm{SCE}}(\boldsymbol{Y}|\boldsymbol{Z})$ is defined as

$$\widetilde{\mathrm{SCE}}(\boldsymbol{Y}|\boldsymbol{Z}) = -\frac{1}{2}\iint p(\boldsymbol{y}|\boldsymbol{z})^2 p(\boldsymbol{z})\mathrm{d}\boldsymbol{z}\mathrm{d}\boldsymbol{y}. \tag{4}$$

Then we have the following theorem (its proof is given in Appendix A), which forms the basis of our proposed method:

Theorem 1

$$\begin{aligned}
\widetilde{\mathrm{SCE}}(\boldsymbol{Y}|\boldsymbol{Z}) - \widetilde{\mathrm{SCE}}(\boldsymbol{Y}|\boldsymbol{X}) &= \frac{1}{2}\iint \left(\frac{p(\boldsymbol{z}_\perp, \boldsymbol{y}|\boldsymbol{z})}{p(\boldsymbol{z}_\perp|\boldsymbol{z})p(\boldsymbol{y}|\boldsymbol{z})} - 1\right)^2 p(\boldsymbol{y}|\boldsymbol{z})^2 p(\boldsymbol{x})\mathrm{d}\boldsymbol{x}\mathrm{d}\boldsymbol{y} \\
&\geq 0.
\end{aligned}$$

This theorem shows $\widetilde{\mathrm{SCE}}(\boldsymbol{Y}|\boldsymbol{Z}) \geq \widetilde{\mathrm{SCE}}(\boldsymbol{Y}|\boldsymbol{X})$, and the equality holds if and only if

$$p(\boldsymbol{z}_\perp, \boldsymbol{y}|\boldsymbol{z}) = p(\boldsymbol{z}_\perp|\boldsymbol{z})p(\boldsymbol{y}|\boldsymbol{z}).$$

This is equivalent to the conditional independence (1), and therefore sufficient dimensionality reduction can be performed by minimizing $\widetilde{\mathrm{SCE}}(\boldsymbol{Y}|\boldsymbol{Z})$ with respect to $\boldsymbol{W}$:

$$\boldsymbol{W}^* = \underset{\boldsymbol{W}\in\mathbb{G}_{d_{\boldsymbol{z}}}^{d_{\boldsymbol{x}}}(\mathbb{R})}{\operatorname{argmin}}\ \widetilde{\mathrm{SCE}}(\boldsymbol{Y}|\boldsymbol{Z} = \boldsymbol{W}\boldsymbol{X}). \tag{5}$$

Here, $\mathbb{G}_{d_{\boldsymbol{z}}}^{d_{\boldsymbol{x}}}(\mathbb{R})$ denotes the *Grassmann manifold*, which is a set of orthogonal matrices without overlaps:

$$\mathbb{G}_{d_{\boldsymbol{z}}}^{d_{\boldsymbol{x}}}(\mathbb{R}) = \{\boldsymbol{W} \in \mathbb{R}^{d_{\boldsymbol{z}} \times d_{\boldsymbol{x}}} \mid \boldsymbol{W}\boldsymbol{W}^\top = \boldsymbol{I}_{d_{\boldsymbol{z}}}\}/\sim,$$

where $\boldsymbol{I}$ denotes the identity matrix and $\sim$ represents the equivalence relation: $\boldsymbol{W}$ and $\boldsymbol{W}'$ are written as $\boldsymbol{W} \sim \boldsymbol{W}'$ if their rows span the same subspace.

Since $p(\boldsymbol{y}|\boldsymbol{z}) = p(\boldsymbol{z},\boldsymbol{y})/p(\boldsymbol{z})$, $\mathrm{SCE}(\boldsymbol{Y}|\boldsymbol{Z})$ is equivalent to the negative *Pearson divergence* (Pearson, 1900) from $p(\boldsymbol{z},\boldsymbol{y})$ to $p(\boldsymbol{z})$, which is a member of the *f-divergence* class (Ali and Silvey, 1966; Csiszár, 1967) with the squared-loss function. On the other hand, ordinary conditional entropy (CE), defined by

$$\mathrm{CE}(\boldsymbol{Y}|\boldsymbol{Z}) = -\iint p(\boldsymbol{z},\boldsymbol{y}) \log p(\boldsymbol{y}|\boldsymbol{z}) \mathrm{d}\boldsymbol{z}\mathrm{d}\boldsymbol{y},$$

is the negative *Kullback-Leibler divergence* (Kullback and Leibler, 1951) from $p(\boldsymbol{z},\boldsymbol{y})$ to $p(\boldsymbol{z})$. Since the Kullback-Leibler divergence is also a member of the f-divergence class (with the log-loss function), CE and SCE have similar properties. Indeed, the above theorem also holds for ordinary CE. However, the Pearson divergence is shown to be more robust against outliers (Basu et al., 1998; Sugiyama et al., 2012), since the log function—which is very sharp near zero—is not included. Furthermore, as shown below, $\widetilde{\mathrm{SCE}}$ can be approximated *analytically* and thus its derivative can also be easily computed. This is a critical property for developing a dimensionality reduction method because we want to minimize $\widetilde{\mathrm{SCE}}$ with respect to $\boldsymbol{W}$, where the gradient is highly useful in devising an optimization algorithm. For this reason, we adopt SCE instead of CE below.

2.3 SCE Approximation

Since $\widetilde{\mathrm{SCE}}(\boldsymbol{Y}|\boldsymbol{Z})$ in Eq.(5) is unknown in practice, we approximate it using samples $\{(\boldsymbol{z}_i,\boldsymbol{y}_i) \mid \boldsymbol{z}_i = \boldsymbol{W}\boldsymbol{x}_i\}_{i=1}^n$.

The trivial inequality $(a-b)^2/2 \geq 0$ yields $a^2/2 \geq ab - b^2/2$, and thus we have

$$\frac{a^2}{2} = \max_b \left[ab - \frac{b^2}{2}\right]. \tag{6}$$

If we set $a = p(\boldsymbol{y}|\boldsymbol{z})$, we have

$$\frac{p(\boldsymbol{y}|\boldsymbol{z})^2}{2} \geq \max_b \left[p(\boldsymbol{y}|\boldsymbol{z})b(\boldsymbol{z},\boldsymbol{y}) - \frac{b(\boldsymbol{z},\boldsymbol{y})^2}{2}\right].$$

If we multiply both sides of the above inequality with $-p(\boldsymbol{z})$, and integrated over $\boldsymbol{z}$ and $\boldsymbol{y}$, we have

$$\widetilde{\mathrm{SCE}}(\boldsymbol{Y}|\boldsymbol{Z}) \leq \min_b \iint \left[\frac{b(\boldsymbol{z},\boldsymbol{y})^2 p(\boldsymbol{z})}{2} - b(\boldsymbol{z},\boldsymbol{y})p(\boldsymbol{z},\boldsymbol{y})\right] \mathrm{d}\boldsymbol{z}\mathrm{d}\boldsymbol{y}, \tag{7}$$

where minimization with respect to b is now performed as a function of $\boldsymbol{z}$ and $\boldsymbol{y}$. For more general discussions on divergence bounding, see Keziou (2003) and Nguyen et al. (2010).

Let us consider a linear-in-parameter model for b:

$$b(\boldsymbol{z}, \boldsymbol{y}) = \boldsymbol{\alpha}^\top \boldsymbol{\varphi}(\boldsymbol{z}, \boldsymbol{y}),$$

where $\boldsymbol{\alpha}$ is a parameter vector and $\boldsymbol{\varphi}(\boldsymbol{z}, \boldsymbol{y})$ is a vector of basis functions. If the expectations over densities $p(\boldsymbol{z})$ and $p(\boldsymbol{z}, \boldsymbol{y})$ are approximated by samples averages and the ℓ_2-regularizer $\lambda \boldsymbol{\alpha}^\top \boldsymbol{\alpha}/2$ ($\lambda \geq 0$) is included, the above minimization problem yields

$$\widehat{\boldsymbol{\alpha}} = \operatorname*{argmin}_{\boldsymbol{\alpha}} \left[\frac{1}{2} \boldsymbol{\alpha}^\top \widehat{\boldsymbol{G}} \boldsymbol{\alpha} - \widehat{\boldsymbol{h}}^\top \boldsymbol{\alpha} + \frac{\lambda}{2} \boldsymbol{\alpha}^\top \boldsymbol{\alpha} \right],$$

where

$$\begin{aligned} \widehat{\boldsymbol{G}} &= \frac{1}{n} \sum_{i=1}^{n} \bar{\boldsymbol{\Phi}}(\boldsymbol{z}_i), \\ \widehat{\boldsymbol{h}} &= \frac{1}{n} \sum_{i=1}^{n} \boldsymbol{\varphi}(\boldsymbol{z}_i, \boldsymbol{y}_i), \\ \bar{\boldsymbol{\Phi}}(\boldsymbol{z}) &= \int \boldsymbol{\varphi}(\boldsymbol{z}, \boldsymbol{y}) \boldsymbol{\varphi}(\boldsymbol{z}, \boldsymbol{y})^\top \mathrm{d}\boldsymbol{y}. \end{aligned} \tag{8}$$

The solution $\widehat{\boldsymbol{\alpha}}$ is analytically given by

$$\widehat{\boldsymbol{\alpha}} = \left(\widehat{\boldsymbol{G}} + \lambda \boldsymbol{I} \right)^{-1} \widehat{\boldsymbol{h}},$$

which yields $\widehat{b}(\boldsymbol{z}, \boldsymbol{y}) = \widehat{\boldsymbol{\alpha}}^\top \boldsymbol{\varphi}(\boldsymbol{z}, \boldsymbol{y})$. Then, from Eq.(7), an approximator of $\widetilde{\mathrm{SCE}}(\boldsymbol{Y}|\boldsymbol{Z})$ is obtained analytically as

$$\widehat{\mathrm{SCE}}(\boldsymbol{Y}|\boldsymbol{Z}) = \frac{1}{2} \widehat{\boldsymbol{\alpha}}^\top \widehat{\boldsymbol{G}} \widehat{\boldsymbol{\alpha}} - \widehat{\boldsymbol{h}}^\top \widehat{\boldsymbol{\alpha}}.$$

We call this method *least-squares conditional entropy* (LSCE).

2.4 Model Selection by Cross-Validation

The above $\widetilde{\mathrm{SCE}}$ approximator depends on the choice of models, i.e., the basis function $\boldsymbol{\varphi}(\boldsymbol{z}, \boldsymbol{y})$ and the regularization parameter λ. Such a model can be objectively selected by cross-validation as follows:

1. The training dataset $\mathcal{S} = \{(\boldsymbol{x}_i, \boldsymbol{y}_i)\}_{i=1}^n$ is divided into K disjoint subsets $\{\mathcal{S}_j\}_{j=1}^K$ with (approximately) the same size.

2. **For** each model M in the candidate set,

(a) **For** $j = 1, \ldots, K$,

i. For model M, the LSCE solution $\widehat{b}^{(M,j)}$ is computed from $\mathcal{S}\backslash\mathcal{S}_j$ (i.e., all samples except $\mathcal{S}_j$).

ii. Evaluate the upper bound of $\widetilde{\mathrm{SCE}}$ obtained by $\widehat{b}^{(M,j)}$ using the hold-out data $\mathcal{S}_j$:

$$\mathrm{CV}_j(M) = \frac{1}{2|\mathcal{S}_j|}\sum_{\boldsymbol{z}\in\mathcal{S}_j}\int \widehat{b}^{(M,j)}(\boldsymbol{z},\boldsymbol{y})^2 \mathrm{d}\boldsymbol{y} - \frac{1}{|\mathcal{S}_j|}\sum_{(\boldsymbol{z},\boldsymbol{y})\in\mathcal{S}_j}\widehat{b}^{(M,j)}(\boldsymbol{z},\boldsymbol{y}),$$

where $|\mathcal{S}_j|$ denotes the cardinality of $\mathcal{S}_j$.

(b) The average score is computed as

$$\mathrm{CV}(M) = \frac{1}{K}\sum_{j=1}^{K}\mathrm{CV}_j(M).$$

3. The model that minimizes the average score is chosen:

$$\widehat{M} = \operatorname*{argmin}_M \mathrm{CV}(M).$$

4. For the chosen model $\widehat{M}$, the LSCE solution $\widehat{b}$ is computed from all samples $\mathcal{S}$ and the approximator $\widehat{\mathrm{SCE}}(\boldsymbol{Y}|\boldsymbol{Z})$ is computed.

In the experiments, we use $K = 5$.

2.5 Dimensionality Reduction with SCE

Now we solve the following optimization problem by gradient descent:

$$\operatorname*{argmin}_{\boldsymbol{W}\in\mathbb{G}_{d_{\boldsymbol{z}}}^{d_{\boldsymbol{x}}}(\mathbb{R})} \widehat{\mathrm{SCE}}(\boldsymbol{Y}|\boldsymbol{Z}=\boldsymbol{W}\boldsymbol{X}). \tag{9}$$

As shown in Appendix B, the gradient of $\widehat{\mathrm{SCE}}(\boldsymbol{Y}|\boldsymbol{Z}=\boldsymbol{W}\boldsymbol{X})$ is given by

$$\frac{\partial\widehat{\mathrm{SCE}}}{\partial W_{l,l'}} = \widehat{\boldsymbol{\alpha}}^\top\frac{\partial\widehat{\boldsymbol{G}}}{\partial W_{l,l'}}\left(\frac{3}{2}\widehat{\boldsymbol{\alpha}}-\widehat{\boldsymbol{\beta}}\right) + \frac{\partial\widehat{\boldsymbol{h}}^\top}{\partial W_{l,l'}}(\widehat{\boldsymbol{\beta}}-2\widehat{\boldsymbol{\alpha}}),$$

where $\widehat{\boldsymbol{\beta}} = \left(\widehat{\boldsymbol{G}}+\lambda\boldsymbol{I}\right)^{-1}\widehat{\boldsymbol{G}}\widehat{\boldsymbol{\alpha}}$.

In the Euclidean space, the above gradient gives the steepest direction. However, on a manifold, the *natural gradient* (Amari, 1998) gives the steepest direction.

The natural gradient $\nabla\widehat{\mathrm{SCE}}(\boldsymbol{W})$ at $\boldsymbol{W}$ is the projection of the ordinary gradient $\frac{\partial\widehat{\mathrm{SCE}}}{\partial W_{l,l'}}$ to the tangent space of $\mathbb{G}_{d_{\boldsymbol{z}}}^{d_{\boldsymbol{x}}}(\mathbb{R})$ at $\boldsymbol{W}$. If the tangent space is equipped with the canonical

metric $\langle \boldsymbol{W}, \boldsymbol{W}' \rangle = \frac{1}{2}\mathrm{tr}(\boldsymbol{W}^\top \boldsymbol{W}')$, the natural gradient is given as follows (Edelman et al., 1998):

$$\nabla\widehat{\mathrm{SCE}} = \frac{\partial\widehat{\mathrm{SCE}}}{\partial \boldsymbol{W}} - \frac{\partial\widehat{\mathrm{SCE}}}{\partial \boldsymbol{W}}\boldsymbol{W}^\top\boldsymbol{W} = \frac{\partial\widehat{\mathrm{SCE}}}{\partial \boldsymbol{W}}\boldsymbol{W}_\perp^\top\boldsymbol{W}_\perp,$$

where $\boldsymbol{W}_\perp$ is a $(d_{\mathbf{x}} - d_{\mathbf{z}}) \times d_{\mathbf{x}}$ matrix such that $\left[\boldsymbol{W}^\top, \boldsymbol{W}_\perp^\top\right]$ is an orthogonal matrix.

Then the *geodesic* from $\boldsymbol{W}$ to the direction of the natural gradient $\nabla\widehat{\mathrm{SCE}}$ over $\mathbb{G}_{d_{\mathbf{z}}}^{d_{\mathbf{x}}}(\mathbb{R})$ can be expressed using $t \in \mathbb{R}$ as

$$\boldsymbol{W}_t = \left[\boldsymbol{I}_{d_{\mathbf{z}}} \quad \boldsymbol{O}_{d_{\mathbf{z}},(d_{\mathbf{x}}-d_{\mathbf{z}})}\right] \times \exp\left(-t\begin{bmatrix} \boldsymbol{O}_{d_{\mathbf{z}},d_{\mathbf{z}}} & \frac{\partial\widehat{\mathrm{SCE}}}{\partial \boldsymbol{W}}\boldsymbol{W}_\perp^\top \\ -\boldsymbol{W}_\perp\frac{\partial\widehat{\mathrm{SCE}}}{\partial \boldsymbol{W}}^\top & \boldsymbol{O}_{d_{\mathbf{x}}-d_{\mathbf{z}},d_{\mathbf{x}}-d_{\mathbf{z}}} \end{bmatrix}\right)\begin{bmatrix}\boldsymbol{W} \\ \boldsymbol{W}_\perp\end{bmatrix},$$

where "exp" for a matrix denotes the matrix exponential and $\boldsymbol{O}_{d,d'}$ denotes the $d \times d'$ zero matrix. Note that the derivative $\partial_t \boldsymbol{W}_t$ at $t = 0$ coincides with the natural gradient $\nabla\widehat{\mathrm{SCE}}$; see (Edelman et al., 1998) for details. Thus, line search along the geodesic in the natural gradient direction is equivalent to finding the minimizer from $\{\boldsymbol{W}_t \mid t \geq 0\}$.

Once $\boldsymbol{W}$ is updated, SCE is re-estimated with the new $\boldsymbol{W}$ and gradient descent is performed again. This entire procedure is repeated until $\boldsymbol{W}$ converges. When SCE is re-estimated, performing cross-validation in every step is computationally expensive. In our implementation, we perform cross-validation only once every 5 gradient updates. Furthermore, to find a better local optimal solution, this gradient descent procedure is executed 20 times with randomly chosen initial solutions and the one achieving the smallest value of $\widehat{\mathrm{SCE}}$ is chosen.

2.6 Conditional Density Estimation with SCE

Since the maximum of Eq.(6) is attained at $b = a$ and $a = p(\boldsymbol{y}|\boldsymbol{z})$ in the current derivation, the optimal $b(\boldsymbol{z}, \boldsymbol{y})$ is actually the conditional density $p(\boldsymbol{y}|\boldsymbol{z})$ itself. Therefore, $\widehat{\boldsymbol{\alpha}}^\top\boldsymbol{\varphi}(\boldsymbol{z}, \boldsymbol{y})$ obtained by LSCE is a conditional density estimator. This actually implies that the upper-bound minimization procedure described in Section 2.3 is equivalent to *least-squares conditional density estimation* (LSCDE) (Sugiyama et al., 2010), which minimizes the squared error:

$$\frac{1}{2}\iint\Big(b(\boldsymbol{z}, \boldsymbol{y}) - p(\boldsymbol{y}|\boldsymbol{z})\Big)^2 p(\boldsymbol{z})\mathrm{d}\boldsymbol{z}\mathrm{d}\boldsymbol{y}.$$

Then, in the same way as the original LSCDE, we may post-process the solution $\widehat{\boldsymbol{\alpha}}$ to make the conditional density estimator non-negative and normalized as

$$\widehat{p}(\boldsymbol{y}|\boldsymbol{z} = \widetilde{\boldsymbol{z}}) = \frac{\widetilde{\boldsymbol{\alpha}}^\top\boldsymbol{\varphi}(\widetilde{\boldsymbol{z}}, \boldsymbol{y})}{\int \widetilde{\boldsymbol{\alpha}}^\top\boldsymbol{\varphi}(\widetilde{\boldsymbol{z}}, \boldsymbol{y}')\mathrm{d}\boldsymbol{y}'}, \tag{10}$$

where $\widetilde{\alpha}_l = \max(\widehat{\alpha}_l, 0)$. Note that, even if the solution is post-processed as Eq.(10), the optimal estimation rate of the LSCDE solution is still maintained (Sugiyama et al., 2010).

2.7 Basis Function Design

In practice, we use the following Gaussian function as the k-th basis:

$$\varphi_k(\boldsymbol{z}, \boldsymbol{y}) = \exp\left(-\frac{\|\boldsymbol{z} - \boldsymbol{u}_k\|^2 + \|\boldsymbol{y} - \boldsymbol{v}_k\|^2}{2\sigma^2}\right), \tag{11}$$

where $(\boldsymbol{u}_k, \boldsymbol{v}_k)$ denotes the k-th Gaussian center located at $(\boldsymbol{z}_k, \boldsymbol{y}_k)$. When the sample size n is too large, we may use only a subset of samples as Gaussian centers. σ denotes the Gaussian bandwidth, which is chosen by cross-validation as explained in Section 2.4. We may use different bandwidths for $\boldsymbol{z}$ and $\boldsymbol{y}$, but this will increase the computation time for model selection. In our implementation, we normalize each element of $\boldsymbol{z}$ and $\boldsymbol{y}$ to have the unit variance in advance and then use the common bandwidth for $\boldsymbol{z}$ and $\boldsymbol{y}$.

A notable advantage of using the Gaussian function is that the integral over $\boldsymbol{y}$ appeared in $\bar{\boldsymbol{\Phi}}(\boldsymbol{z})$ (see Eq.(8)) can be computed analytically as

$$\bar{\Phi}_{k,k'}(\boldsymbol{z}) = (\sqrt{\pi}\sigma)^{d_{\mathcal{Y}}} \ \exp\left(-\frac{2\|\boldsymbol{z} - \boldsymbol{u}_k\|^2 + 2\|\boldsymbol{z} - \boldsymbol{u}_{k'}\|^2 + \|\boldsymbol{v}_k - \boldsymbol{v}_{k'}\|^2}{4\sigma^2}\right).$$

Similarly, the normalization term in Eq.(10) can also be computed analytically as

$$\int \widetilde{\boldsymbol{\alpha}}^\top \boldsymbol{\varphi}(\boldsymbol{z}, \boldsymbol{y}) \mathrm{d}\boldsymbol{y} = (\sqrt{2\pi}\sigma)^{d_{\mathcal{Y}}} \sum_k \widetilde{\alpha}_k \exp\left(-\frac{\|\boldsymbol{z} - \boldsymbol{u}_k\|^2}{2\sigma^2}\right).$$

2.8 Discussions

We have proposed to minimize SCE for dimensionality reduction:

$$\mathrm{SCE}(\boldsymbol{Y}|\boldsymbol{Z}) = -\frac{1}{2}\iint \left(\frac{p(\boldsymbol{z}, \boldsymbol{y})}{p(\boldsymbol{z})} - 1\right)^2 p(\boldsymbol{z}) \mathrm{d}\boldsymbol{z} \mathrm{d}\boldsymbol{y}.$$

On the other hand, in the previous work (Suzuki and Sugiyama, 2013), *squared-loss mutual information* (SMI) was maximized for dimensionality reduction:

$$\mathrm{SMI}(\boldsymbol{Y}, \boldsymbol{Z}) = \frac{1}{2}\iint \left(\frac{p(\boldsymbol{z}, \boldsymbol{y})}{p(\boldsymbol{z})p(\boldsymbol{y})} - 1\right)^2 p(\boldsymbol{z})p(\boldsymbol{y}) \mathrm{d}\boldsymbol{z} \mathrm{d}\boldsymbol{y}.$$

This shows that the essential difference is whether $p(\boldsymbol{y})$ is included in the denominator of the density ratio. Thus, if $p(\boldsymbol{y})$ is uniform, the proposed dimensionality reduction method using SCE is reduced to the existing method using SMI. However, if $p(\boldsymbol{y})$ is not uniform, the density ratio function $\frac{p(\boldsymbol{z},\boldsymbol{y})}{p(\boldsymbol{z})p(\boldsymbol{y})}$ included in SMI may be more fluctuated than $\frac{p(\boldsymbol{z},\boldsymbol{y})}{p(\boldsymbol{z})}$ included in SCE. Since a smoother function can be more accurately estimated from a small number of samples in general, the proposed method using SCE is expected to work better than the existing method using SMI. We will experimentally demonstrate this effect in Section 3.

Sufficient dimension reduction based on the conditional density $p(\boldsymbol{y}|\boldsymbol{z})$ has also been studied in statistic literatures. The *density-minimum average variance estimation* (dMAVE) method (Xia, 2007) finds a dimension reduction subspace using local linear regression for the conditional density in a semi-parametric manner. A similar approach has also been taken in the *sliced regression for dimension reduction* method (Wang and Xia, 2008), where the cumulative conditional density is used instead of the conditional density. A Bayesian approach to sufficient dimension reduction called the *Bayesian dimension reduction* (BDR) method (Reich et al., 2011) has been proposed recently. This method models the conditional density as a Gaussian mixture model and obtains a dimension reduction subspace through sampling from the learned prior distribution of low-dimensional input. These methods have shown to work well for dimension reduction in real-world datasets, although they are applicable only to univariate output data where $d_{\mathbf{y}} = 1$.

In regression, learning with the squared-loss is not robust against outliers (Huber, 1981). However, density estimation (Basu et al., 1998) and density ratio estimation (Sugiyama et al., 2012) under the Pearson divergence is known to be robust against outliers. Thus, in the same sense, the proposed LSCE estimator would also be robust against outliers. We will experimentally investigate the robustness in Section 3.

3 Experiments

In this section, we experimentally investigate the practical usefulness of the proposed method. We consider the following dimensionality reduction schemes:

None: No dimensionality reduction is performed.

dMAVE: The density-minimum average variance estimation method where dimension reduction is performed through local linear regression for the conditional density[1] (Xia, 2007).

BDR: The Bayesian dimension reduction method where the conditional density is modeled by a Gaussian mixture model and dimension reduction is performed by sampling from the prior distribution of low-dimensional input[2] (Reich et al., 2011).

LSMI: Dimension reduction is performed by maximizing an SMI approximator called *least-squares MI* (LSMI) using natural gradients over the Grassmann manifold (Suzuki and Sugiyama, 2013).

LSCE (proposed): Dimension reduction is performed by minimizing the proposed LSCE using natural gradients over the Grassmann manifold.

True (reference) The "true" subspace is used (only for artificial data).

[1] We use the program code provided by the author.

[2] We use the program code available at "`http://www4.stat.ncsu.edu/~reich/code/BayesSDR.R`".

After dimension reduction, we execute the following conditional density estimators:

ϵ-KDE: ϵ-neighbor kernel density estimation, where ϵ is chosen by least-squares cross-validation.

LSCDE: Least-squares conditional density estimation (Sugiyama et al., 2010).

Note that the proposed method, which is the combination of LSCE and LSCDE, does not explicitly require the post-LSCDE step because LSCDE is executed inside LSCE. Since the dMAVE and BDR methods are applicable only to univariate output, they are not included in experiments with multivariate output data.

3.1 Illustration

First, we illustrate the behavior of the plain LSCDE (None/LSCDE) and the proposed method (LSCE/LSCDE). The datasets illustrated in Figure 2 have $d_{\mathbf{x}} = 5$, $d_{\mathbf{y}} = 1$, and $d_{\mathbf{z}} = 1$. The first dimension of input $\boldsymbol{x}$ and output y of the samples are plotted in the graphs, and other 4 dimensions of $\boldsymbol{x}$ are just standard normal noise. The results show that the plain LSCDE does not perform well due to the irrelevant noise dimensions of $\boldsymbol{x}$, while the proposed method gives much better estimates.

3.2 Artificial Datasets

Next, we compare the proposed method with the existing dimensionality reduction methods on conditional density estimation by LSCDE in artificial datasets.

For $d_{\mathbf{x}} = 5$, $d_{\mathbf{y}} = 1$, $\boldsymbol{x} \sim \mathcal{N}(\boldsymbol{x}|\mathbf{0}, \boldsymbol{I}_5)$, and $\epsilon \sim \mathcal{N}(\epsilon|0, 0.25^2)$, where $\mathcal{N}(\cdot|\boldsymbol{\mu}, \boldsymbol{\Sigma})$ denotes the normal distribution with mean $\boldsymbol{\mu}$ and covariance matrix $\boldsymbol{\Sigma}$, we consider the following artificial datasets:

(a) $d_{\mathbf{z}} = 2$ and $y = (x^{(1)})^2 + (x^{(2)})^2 + \epsilon$.

(b) $d_{\mathbf{z}} = 1$ and $y = x^{(2)} + (x^{(2)})^2 + (x^{(2)})^3 + \epsilon$.

(c) $d_{\mathbf{z}} = 1$ and $y = \begin{cases} (x^{(1)})^2 + \epsilon & \text{with 0.85 probability,} \\ 2\epsilon - 4 & \text{with 0.15 probability.} \end{cases}$

The first row of Figure 3 shows the dimensionality reduction error between true $\boldsymbol{W}^*$ and its estimate $\widehat{\boldsymbol{W}}$ for different sample size n, measured by

$$\mathrm{Error}_{\mathrm{DR}} = \|\widehat{\boldsymbol{W}}^\top \widehat{\boldsymbol{W}} - \boldsymbol{W}^{*\top} \boldsymbol{W}^*\|_{\mathrm{Frobenius}},$$

where $\|\cdot\|_{\mathrm{Frobenius}}$ denotes the Frobenius norm. All methods perform similarly for the dataset (a), and the dMAVE and BDR methods outperform LSCE and LSMI when $n = 50$.

In the dataset (b), LSMI does not work well compare to other methods especially when $n \geq 250$. To explain this behavior, we plot the histograms of $\{y\}_{i=1}^{400}$ in the left column of Figure 4. They show that the profile of the histogram (which is a sample

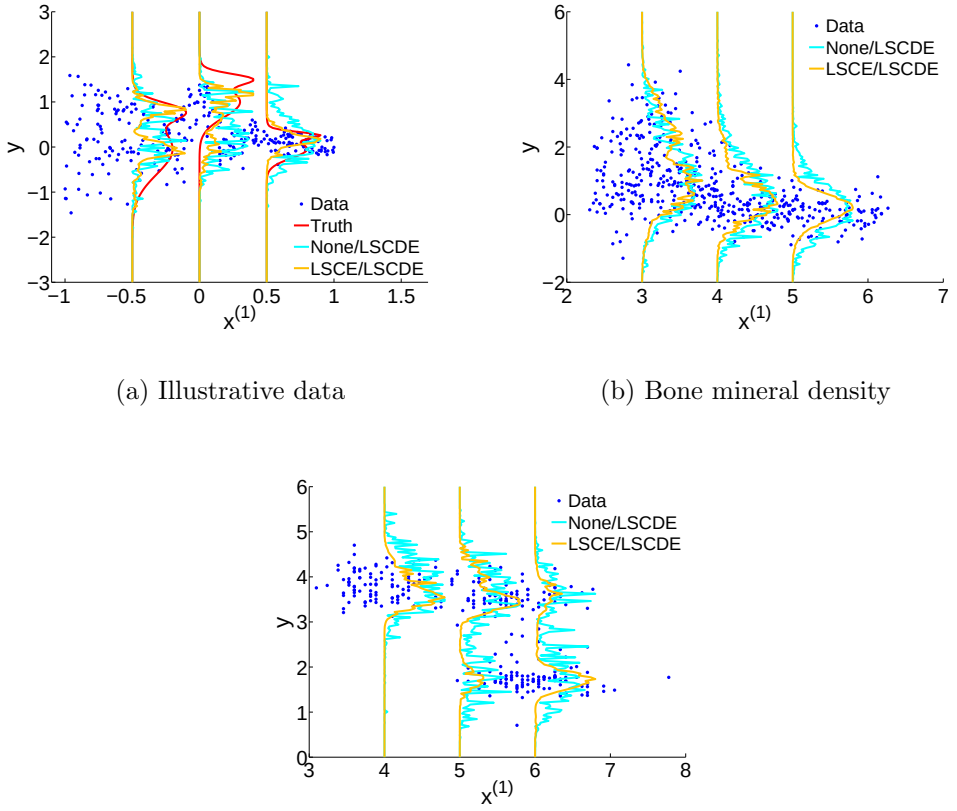

(a) Illustrative data

(b) Bone mineral density

(c) Old faithful geyser

Figure 2: Examples of conditional density estimation by plain LSCDE (None/LSCDE) and the proposed method (LSCE/LSCDE).

approximation of $p(y)$) in the dataset (b) is much sharper than that in the dataset (a). As discussed in Section 2.8, the density ratio $\frac{p(\boldsymbol{z},y)}{p(\boldsymbol{z})p(\boldsymbol{y})}$ used in LSMI contains $p(\boldsymbol{y})$. Thus, for the dataset (b), the density ratio $\frac{p(\boldsymbol{z},y)}{p(\boldsymbol{z})p(\boldsymbol{y})}$ would be highly non-smooth and thus is hard to approximate. On the other hand, the conditional density used in other methods is $\frac{p(\boldsymbol{z},y)}{p(\boldsymbol{z})}$, where $p(\boldsymbol{y})$ is not included. Therefore, $\frac{p(\boldsymbol{z},y)}{p(\boldsymbol{z})}$ would be smoother than $\frac{p(\boldsymbol{z},y)}{p(\boldsymbol{z})p(\boldsymbol{y})}$ and $\frac{p(\boldsymbol{z},y)}{p(\boldsymbol{z})}$ is easier to estimate than $\frac{p(\boldsymbol{z},y)}{p(\boldsymbol{z})p(\boldsymbol{y})}$.

For the dataset (c), we consider the situation where $\{y_i\}_{i=1}^n$ contain outliers which are not related to $\boldsymbol{x}$. The data profile of dataset (c) in the right column of Figure 4 illustrates such a situation. The result on dataset (c) shows that the proposed LSCE method is robust against outliers and gives the best subspace estimation accuracy, while the BDR method performs unreliably with large standard errors.

The right column of Figure 3 plots the conditional density estimation error between

true $p(\boldsymbol{y}|\boldsymbol{x})$ and its estimate $\widehat{p}(\boldsymbol{y}|\boldsymbol{x})$, evaluated by the squared-loss:

$$\mathrm{Error}_{\mathrm{CDE}} = \frac{1}{2n'}\sum_{i=1}^{n'}\int \widehat{p}(\boldsymbol{y}|\widetilde{\boldsymbol{x}}_i)^2 \mathrm{d}\boldsymbol{y} - \frac{1}{n'}\sum_{i=1}^{n'}\widehat{p}(\widetilde{\boldsymbol{y}}_i|\widetilde{\boldsymbol{x}}_i),$$

where $\{(\widetilde{\boldsymbol{x}}_i, \widetilde{\boldsymbol{y}}_i)\}_{i=1}^{n'}$ is a set of test samples that have not been used for training. We set $n' = 1000$. For the dataset (a) and (c), all methods with dimension reduction perform equally well, which are much better than no dimension reduction (None/LSCDE) and are comparable to the method with the true subspace (True/LSCDE). For the dataset (b), all method except LSMI/LSCDE perform well overall and comparable to the method with the true subspace.

3.3 Benchmark Datasets

Next, we use the UCI benchmark datasets (Bache and Lichman, 2013). We randomly select n samples from each dataset for training, and the rest are used to measure the conditional density estimation error in the test phase. Since the dimensionality of the subspace $d_{\mathbf{z}}$ is unknown, we chose it by cross-validation. More specifically, 5-fold cross-validation is performed for each combination of the dimensionality reduction and conditional density estimation methods to choose subspace dimensionalities $d_{\mathbf{z}}$ such that the conditional density estimation error is minimized. Note that tuning parameters λ and σ are also chosen based on cross-validation for each method. Since the conditional density estimation error is equivalent to SCE, choosing the subspace dimensionalities by the conditional density estimation error in LSCE is equivalent to choosing subspace dimensionalities which gives the minimum SCE value.

The results of univariate output benchmark datasets averaged over 10 runs are summarized in Table 1, showing that LSCDE tends to outperform ϵ-KDE and the proposed LSCE/LSCDE method works well overall. Both LSMI/LSCDE and dMAVE/LSCDE methods also perform well in all datasets, while BDR/LSCDE does not work well in the datasets containing outliers such as "Red Wine", "White Wine", and "Forest Fires". Table 2 describes the subspace dimensionalities chosen by cross-validation averaged over 10 runs. It shows that all dimensionality reduction methods reduce the input dimension significantly, especially for "Yacht", "Red Wine", and "White Wine" where the best method always chooses $d_{\mathbf{z}} = 1$ in all runs.

The result of multivariate output "Stock" and "Energy" benchmark datasets are summarized in Table 3, showing that the proposed LSCE/LSCDE method also works well for multivariate output datasets and significantly outperforms methods without dimensionality reduction. Table 4 describes the subspace dimensionalities selected by cross-validation, showing that LSMI/LSCDE tends to more aggressively reduce the dimensionality than LSCE/LSCDE.

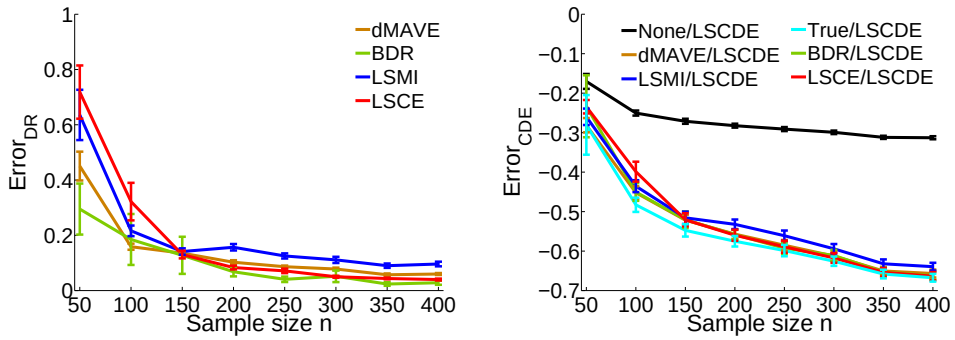

(a) Artificial data 1

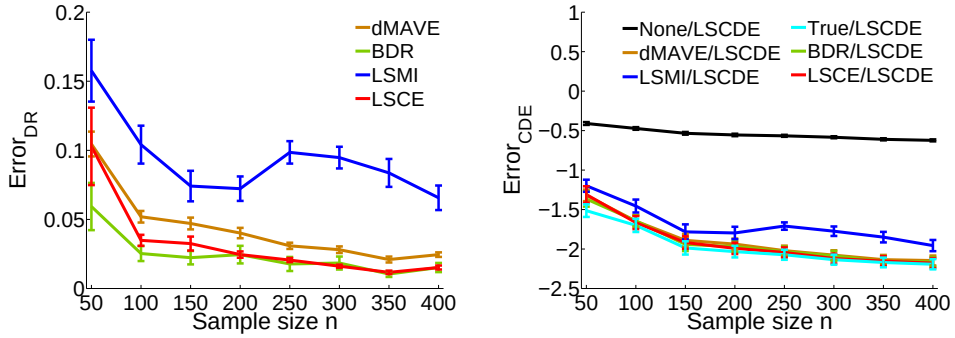

(b) Artificial data 2

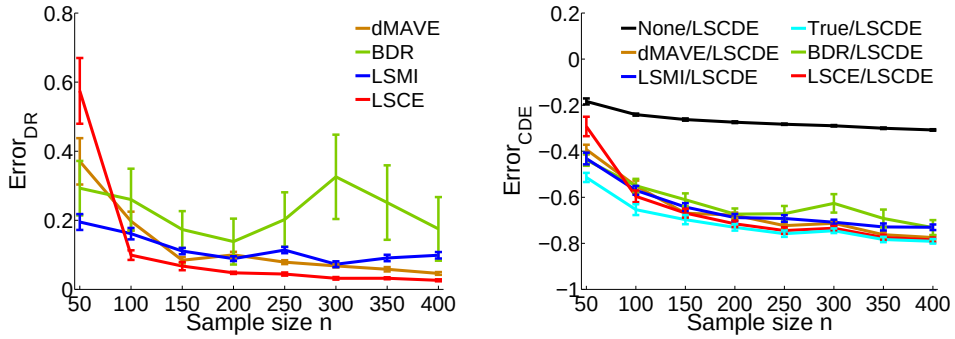

(c) Artificial data 3

Figure 3: Left column: The mean and standard error of the dimensionality reduction error over 20 runs. Right column: The mean and standard error of the conditional density estimation error over 20 runs.

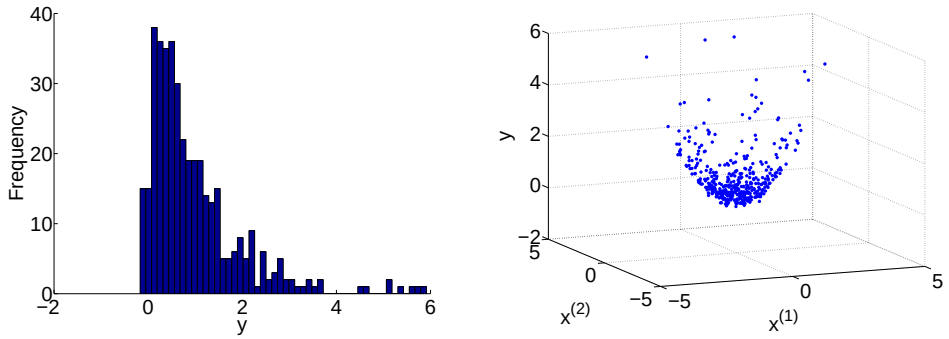

(a) Artificial data 1

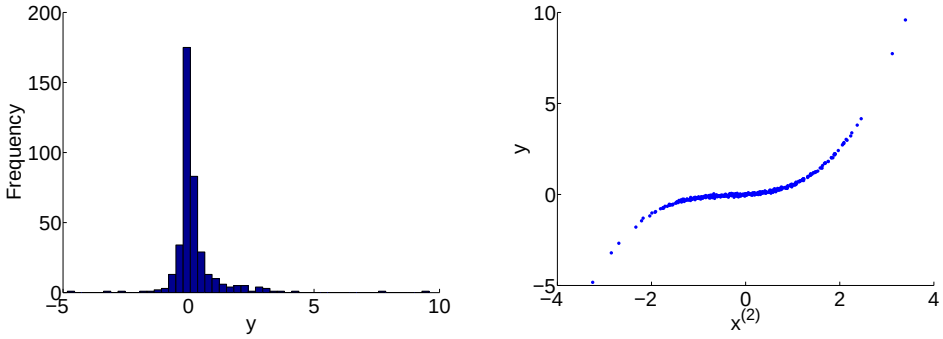

(b) Artificial data 2

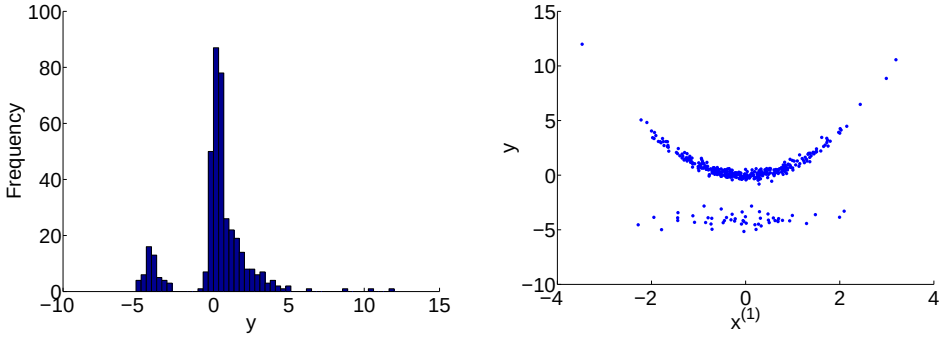

(c) Artificial data 3

Figure 4: Left column: Example histograms of $\{y_i\}_{i=1}^{400}$ on the artificial datasets. Right column: Example data plot of relevant features of $\boldsymbol{x}$ against y when $n = 400$ on the artificial datasets. The left distribution in the histogram of dataset (c) is regarded as outliers.

Table 1: Mean and standard error of the conditional density estimation error over 10 runs for univariate output datasets. The best method in term of the mean error and comparable methods according to the two-sample paired *t-test* at the significance level 5% are specified by bold face.

Dataset	LSCE		LSMI		dMAVE		BDR		No reduction	
	LSCDE	ϵ-KDE	LSCDE	ϵ-KDE	LSCDE	ϵ-KDE	LSCDE	ϵ-KDE	LSCDE	ϵ-KDE
Servo	**−2.95(.17)**	**−3.03(.14)**	−2.69(.18)	**−2.95(.11)**	**−3.13(.13)**	**−3.17(.10)**	**−2.96(.10)**	**−2.95(.12)**	−2.62(.09)	−2.72(.06)
Yacht	**−6.46(.02)**	**−6.30(.14)**	−5.63(.26)	−5.47(.29)	−6.25(.06)	−5.97(.12)	**−6.45(.04)**	−6.05(.18)	−1.72(.04)	−2.95(.02)
Auto MPG	−1.80(.04)	−1.75(.05)	−1.85(.04)	−1.77(.05)	**−1.98(.04)**	**−1.97(.04)**	**−1.91(.04)**	−1.84(.05)	−1.75(.04)	−1.46(.04)
Concrete	**−1.37(.03)**	−1.18(.06)	**−1.30(.03)**	−1.18(.04)	**−1.42(.06)**	−1.15(.05)	**−1.37(.04)**	−1.10(.04)	−1.11(.02)	−0.80(.03)
Physicochem	**−1.19(.01)**	−0.99(.02)	**−1.20(.01)**	−0.97(.02)	−1.17(.01)	−0.93(.02)	−1.13(.02)	−0.96(.02)	**−1.19(.01)**	−0.91(.01)
Red Wine	**−2.85(.02)**	−1.95(.17)	**−2.82(.03)**	−1.93(.17)	**−2.82(.02)**	−1.93(.20)	−2.66(.03)	−2.18(.14)	−2.03(.02)	−1.13(.04)
White Wine	**−2.31(.01)**	**−2.47(.15)**	**−2.35(.02)**	**−2.60(.12)**	−2.17(.01)	**−2.65(.20)**	−1.97(.02)	−1.91(.02)	−2.06(.01)	−1.89(.01)
Forest Fires	**−7.18(.02)**	−6.91(.03)	−6.93(.04)	−6.96(.02)	−7.10(.03)	−6.93(.04)	−7.08(.03)	−6.97(.01)	−3.40(.07)	−6.96(.02)
Housing	**−1.72(.09)**	−1.58(.08)	**−1.91(.05)**	−1.62(.08)	**−1.76(.11)**	−1.50(.13)	**−1.86(.09)**	−1.74(.03)	−1.41(.05)	−1.13(.01)

Table 2: Mean and standard error of the chosen subspace dimensionality over 10 runs for univariate output datasets.

Data set	$(d_{\mathbf{x}}, d_{\mathbf{y}})$	n	LSCE		LSMI		dMAVE		BDR	
			LSCDE	ϵ-KDE	LSCDE	ϵ-KDE	LSCDE	ϵ-KDE	LSCDE	ϵ-KDE
Servo	$(4, 1)$	50	1.6(0.27)	2.4(0.40)	2.2(0.33)	1.6(0.31)	1.5(0.22)	1.5(0.31)	1.2(0.13)	2.0(0.37)
Yacht	$(6, 1)$	80	1.0(0)	1.0(0)	1.0(0)	1.0(0)	1.2(0.13)	1.0(0)	1.0(0)	1.0(0)
Auto MPG	$(7, 1)$	100	3.2(0.66)	1.3(0.15)	2.1(0.67)	1.1(0.10)	1.5(0.22)	1.0(0)	1.4(0.16)	1.2(0.13)
Concrete	$(8, 1)$	300	1.0(0)	1.0(0)	1.2(0.13)	1.0(0)	1.7(0.15)	1.0(0)	2.3(0.21)	1.0(0)
Physicochem	$(9, 1)$	500	6.5(0.58)	1.9(0.28)	6.6(0.58)	2.6(0.86)	7.5(0.48)	5.0(1.33)	2.6(0.16)	1.7(0.26)
Red Wine	$(11, 1)$	300	1.0(0)	1.3(0.15)	1.2(0.20)	1.0(0)	1.0(0)	1.1(0.10)	1.5(0.22)	1.0(0)
White Wine	$(11, 1)$	400	1.2(0.13)	1.0(0)	1.4(0.31)	1.0(0)	1.8(0.70)	1.0(0)	3.1(0.23)	2.7(0.30)
Forest Fires	$(12, 1)$	100	1.2(0.20)	4.4(0.87)	1.4(0.22)	5.6(1.25)	1.5(0.27)	5.2(1.31)	1.2(0.20)	2.8(0.33)
Housing	$(13, 1)$	100	3.9(0.74)	1.9(0.80)	2.0(0.39)	1.3(0.15)	3.0(0.77)	1.2(0.13)	1.6(0.22)	1.0(0)

Table 3: Mean and standard error of the conditional density estimation error over 10 runs for multivariate output datasets. The best method in term of the mean error and comparable methods according to the two-sample paired *t-test* at the significance level 5% are specified by bold face.

Dataset	LSCE		LSMI		No reduction		Scale
	LSCDE	ϵ-KDE	LSCDE	ϵ-KDE	LSCDE	ϵ-KDE	
Stock	$-8.37(0.53)$	$\mathbf{-9.75(0.37)}$	$\mathbf{-9.42(0.50)}$	$\mathbf{-10.27(0.33)}$	$-7.35(0.13)$	$-9.25(0.14)$	$\times 1$
Energy	$\mathbf{-7.13(0.04)}$	$-4.18(0.22)$	$-6.04(0.47)$	$-3.41(0.49)$	$-2.12(0.06)$	$-1.95(0.14)$	$\times 10$
2 Joints	$\mathbf{-10.49(0.86)}$	$-7.50(0.54)$	$\mathbf{-8.00(0.84)}$	$-7.44(0.60)$	$-3.95(0.13)$	$-3.65(0.14)$	$\times 1$
4 Joints	$\mathbf{-2.81(0.21)}$	$-1.73(0.14)$	$-2.06(0.25)$	$-1.38(0.16)$	$-0.83(0.03)$	$-0.75(0.01)$	$\times 10$
9 Joints	$\mathbf{-8.37(0.83)}$	$-2.44(0.17)$	$\mathbf{-9.74(0.63)}$	$-2.37(0.51)$	$-1.60(0.36)$	$-0.89(0.02)$	$\times 100$
Sumi-e 1	$\mathbf{-9.96(1.60)}$	$-1.49(0.78)$	$\mathbf{-6.00(1.28)}$	$1.24(1.99)$	$-5.98(0.80)$	$-0.17(0.44)$	$\times 10$
Sumi-e 2	$\mathbf{-16.83(1.70)}$	$-2.22(0.97)$	$-9.54(1.31)$	$-3.12(0.75)$	$-7.69(0.62)$	$-0.66(0.13)$	$\times 10$
Sumi-e 3	$\mathbf{-24.92(1.92)}$	$-6.61(1.25)$	$-18.0(2.61)$	$-4.47(0.68)$	$-8.98(0.66)$	$-1.45(0.43)$	$\times 10$

Table 4: Mean and standard error of the chosen subspace dimensionality over 10 runs for multivariate output datasets.

Data set	$(d_{\mathbf{x}}, d_{\mathbf{y}})$	n	LSCE		LSMI	
			LSCDE	ϵ-KDE	LSCDE	ϵ-KDE
Stock	$(7, 2)$	100	3.2(0.83)	2.1(0.59)	2.1(0.60)	2.7(0.67)
Energy	$(8, 2)$	200	5.9(0.10)	3.9(0.80)	2.1(0.10)	2.0(0.30)
2 Joints	$(6, 4)$	100	2.9(0.31)	2.7(0.21)	2.5(0.31)	2.0(0)
4 Joints	$(12, 8)$	200	5.2(0.68)	6.2(0.63)	5.4(0.67)	4.6(0.43)
9 Joints	$(27, 18)$	500	13.8(1.28)	15.3(0.94)	11.4(0.75)	13.2(1.02)
Sumi-e 1	$(9, 6)$	200	5.3(0.72)	2.9(0.85)	4.5(0.45)	3.2(0.76)
Sumi-e 2	$(9, 6)$	250	4.2(0.55)	4.4(0.85)	4.6(0.87)	2.5(0.78)
Sumi-e 3	$(9, 6)$	300	3.6(0.50)	2.7(0.76)	2.6(0.40)	1.6(0.27)

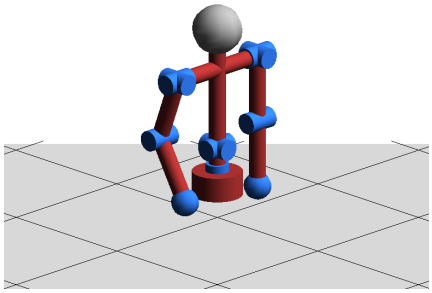

Figure 5: Simulator of the upper-body part of the humanoid robot *CB-i*.

3.4 Humanoid Robot

We evaluate the performance of the proposed method on humanoid robot transition estimation. We use a simulator of the upper-body part of the humanoid robot *CB-i* (Cheng et al., 2007) (see Figure 5). The robot has 9 controllable joints: shoulder pitch, shoulder roll, elbow pitch of the right arm, shoulder pitch, shoulder roll, elbow pitch of the left arm, waist yaw, torso roll, and torso pitch joints.

Posture of the robot is described by 18-dimensional real-valued state vector $\boldsymbol{s}$, which corresponds to the angle and angular velocity of each joint in radians and radians per seconds, respectively. We can control the robot by sending the action command $\boldsymbol{a}$ to the system. The action command $\boldsymbol{a}$ is a 9-dimensional real-valued vector, which corresponds to the target angle of each joint. When the robot is currently at state $\boldsymbol{s}$ and receives action $\boldsymbol{a}$, the physical control system of the simulator calculates the amount of torques to be applied to each joint. These torques are calculated by the *proportional-derivative* (PD) controller as

$$\tau_i = K_{p_i}(a_i - s_i) - K_{d_i}\dot{s}_i,$$

where s_i, $\dot{s}_i$, and a_i denote the current angle, the current angular velocity, and the received target angle of the i-th joint, respectively. K_{p_i} and K_{d_i} denote the position and velocity gains for the i-th joint, respectively. We set $K_{p_i} = 2000$ and $K_{d_i} = 100$ for all joints except that $K_{p_i} = 200$ and $K_{d_i} = 10$ for the elbow pitch joints. After the torques are applied to the joints, the physical control system update the state of the robot to $\boldsymbol{s}'$.

In the experiment, we randomly choose the action vector $\boldsymbol{a}$ and simulate a noisy control system by adding a bimodal Gaussian noise vector. More specifically, the action a_i of the i-th joint is first drawn from uniform distribution on $[s_i - 0.087, s_i + 0.087]$. The drawn action is then contaminated by Gaussian noise with mean 0 and standard deviation 0.034 with probability 0.6 and Gaussian noise with mean -0.087 and standard deviation 0.034 with probability 0.4. By repeatedly control the robot n times, we obtain the transition samples $\{(\boldsymbol{s}_j, \boldsymbol{a}_j, \boldsymbol{s}'_j)\}_{j=1}^n$. Our goal is to learn the system dynamic as a state transition

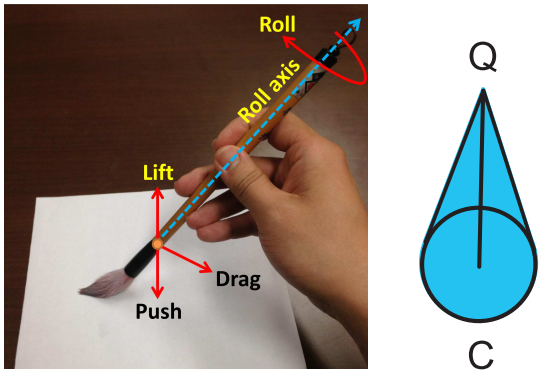

Figure 6: Three actions of the brush, which is modeled as the footprint on a paper canvas.

probability $p(\boldsymbol{s}'|\boldsymbol{s},\boldsymbol{a})$ from these samples. Thus, as the conditional density estimation problem, the state-action pair $(\boldsymbol{s}^\top,\boldsymbol{a}^\top)^\top$ is regarded as input variable $\boldsymbol{x}$, while the next state $\boldsymbol{s}'$ is regarded as output variable $\boldsymbol{y}$. Such state-transition probabilities are highly useful in model-based reinforcement learning (Sutton and Barto, 1998).

We consider three scenarios: Using only 2 joints (right shoulder pitch and right elbow pitch), only 4 joints (in addition, right shoulder roll and waist yaw), and all 9 joints. Thus, $d_{\mathbf{x}} = 6$ and $d_{\mathbf{y}} = 4$ for the 2-joint case, $d_{\mathbf{x}} = 12$ and $d_{\mathbf{y}} = 8$ for the 4-joint case, and $d_{\mathbf{x}} = 27$ and $d_{\mathbf{y}} = 18$ for the 9-joint case. We generate 500, 1000, and 1500 transition samples for the 2-joint, 4-joint, and 9-joint cases. We then randomly choose $n = 100$, 200, and 500 samples for training, and use the rest for evaluating the test error. The results are summarized also in Table 3, showing that the proposed method performs well for the all three cases. Table 4 describes the dimensionalities selected by cross-validation, showing that the humanoid robot's transition is highly redundant.

3.5 Computer Art

Finally, we consider the transition estimation problem in *sumi-e* style brush drawings for non-photorealistic rendering (Xie et al., 2012). Our aim is to learn the brush dynamics as state transition probability $p(\boldsymbol{s}'|\boldsymbol{s},\boldsymbol{a})$ from the real artists' stroke-drawing samples.

From a video of real brush strokes, we extract footprints and identify corresponding 3-dimensional actions (see Figure 6). The state vector consists of six measurements: the angle of the velocity vector and the heading direction of the footprint relative to the medial axis of the drawing shape, the ratio of the offset distance from the center of the footprint to the nearest point on the medial axis over the radius of the footprint, the relative curvatures of the nearest current point and the next point on the medial axis, and the binary signal of the reverse driving or not. Thus, the state transition probability $p(\boldsymbol{s}'|\boldsymbol{s},\boldsymbol{a})$ has 9-dimensional input and 6-dimensional output. We collect 722 transition samples in total. We randomly choose $n = 200, 250$, and 300 for training and use the rest for testing.

The estimation results summarized at the bottom of Table 3 and Table 4. These tables show that there exists a low-dimensional sufficient subspace and the proposed method can

successfully find it.

4 Conclusion

We proposed a new method for conditional density estimation in high-dimension problems. The key idea of the proposed method is to perform sufficient dimensionality reduction by minimizing the square-loss conditional entropy (SCE), which can be estimated by least-squares conditional density estimation. Thus, dimensionality reduction and conditional density estimation are carried out simultaneously in an integrated manner.

We have shown that SCE and the squared-loss mutual information (SMI) are similar but different in that the output density is included in the denominator of the density ratio in SMI. This means that estimation of SMI is hard when the output density is fluctuated, while the proposed method using SCE does not suffer from this problem. The proposed method is also robust against outliers since minimization of the Pearson divergence automatically weights down effects of outlier points. Moreover, the proposed method is applicable to multivariate output data, which is not straightforward to handle in other dimensionality reduction methods based on conditional probability density. The effectiveness of the proposed method was demonstrated through extensive experiments including humanoid robot transition and computer art.

References

Ali, S. M. and Silvey, S. D. (1966). A general class of coefficients of divergence of one distribution from another. *Journal of the Royal Statistical Society, Series B*, 28(1):131–142.

Amari, S. (1998). Natural gradient works efficiently in learning. *Neural Computation*, 10(2):251–276.

Bache, K. and Lichman, M. (2013). UCI machine learning repository.

Basu, A., Harris, I. R., Hjort, N. L., and Jones, M. C. (1998). Robust and efficient estimation by minimising a density power divergence. *Biometrika*, 85(3):pp. 549–559.

Cheng, G., Hyon, S., Morimoto, J., Ude, A., Joshua, G., Colvin, G., Scroggin, W., and Stephen, C. J. (2007). Cb: A humanoid research platform for exploring neuroscience. *Advanced Robotics*, 21(10):1097–1114.

Cook, R. D. and Ni, L. (2005). Sufficient dimension reduction via inverse regression. *Journal of the American Statistical Association*, 100(470):410–428.

Csiszár, I. (1967). Information-type measures of difference of probability distributions and indirect observation. *Studia Scientiarum Mathematicarum Hungarica*, 2:229–318.

Edelman, A., Arias, T. A., and Smith, S. T. (1998). The geometry of algorithms with orthogonality constraints. *SIAM Journal on Matrix Analysis and Applications*, 20(2):303–353.

Fukumizu, K., Bach, F. R., and Jordan, M. I. (2009). Kernel dimension reduction in regression. *The Annals of Statistics*, 37(4):1871–1905.

Huber, P. J. (1981). *Robust Statistics*. Wiley, New York, NY, USA.

Keziou, A. (2003). Dual representation of ϕ-divergences and applications. *Comptes Rendus Mathématique*, 336(10):857–862.

Kullback, S. and Leibler, R. A. (1951). On information and sufficiency. *The Annals of Mathematical Statistics*, 22:79–86.

Li, K. (1991). Sliced inverse regression for dimension reduction. *Journal of the American Statistical Association*, 86(414):316–342.

Nguyen, X., Wainwright, M. J., and Jordan, M. I. (2010). Estimating divergence functionals and the likelihood ratio by convex risk minimization. *IEEE Transactions on Information Theory*, 56(11):5847–5861.

Pearson, K. (1900). On the criterion that a given system of deviations from the probable in the case of a correlated system of variables is such that it can be reasonably supposed to have arisen from random sampling. *Philosophical Magazine Series 5*, 50(302):157–175.

Reich, B. J., Bondell, H. D., and Li, L. (2011). Sufficient dimension reduction via bayesian mixture modeling. *Biometrics*, 67(3):886–895.

Sugiyama, M., Suzuki, T., and Kanamori, T. (2012). Density ratio matching under the Bregman divergence: A unified framework of density ratio estimation. *Annals of the Institute of Statistical Mathematics*, 64(5):1009–1044.

Sugiyama, M., Takeuchi, I., Kanamori, T., Suzuki, T., Hachiya, H., and Okanohara, D. (2010). Conditional density estimation via least-squares density ratio estimation. In Teh, Y. W. and Tiggerington, M., editors, *Proceedings of the Thirteenth International Conference on Artificial Intelligence and Statistics (AISTATS2010)*, volume 9 of *JMLR Workshop and Conference Proceedings*, pages 781–788, Sardinia, Italy.

Sutton, R. S. and Barto, G. A. (1998). *Reinforcement Learning: An Introduction*. MIT Press, Cambridge, MA, USA.

Suzuki, T. and Sugiyama, M. (2013). Sufficient dimension reduction via squared-loss mutual information estimation. *Neural Computation*, 3(25):725–758.

Wang, H. and Xia, Y. (2008). Sliced regression for dimension reduction. *Journal of the American Statistical Association*, 103(482):811–821.

Xia, Y. (2007). A constructive approach to the estimation of dimension reduction directions. *The Annals of Statistics*, 35(6):2654–2690.

Xie, N., Hachiya, H., and Sugiyama, M. (2012). Artist agent: A reinforcement learning approach to automatic stroke generation in oriental ink painting. In Langford, J. and Pineau, J., editors, *Proceedings of 29th International Conference on Machine Learning (ICML2012)*, pages 153–160, Edinburgh, Scotland.

A Proof of Theorem 1

The $\widetilde{\mathrm{SCE}}$ is defined as

$$\widetilde{\mathrm{SCE}}(\boldsymbol{Y}|\boldsymbol{Z}) = -\frac{1}{2}\iint p(\boldsymbol{y}|\boldsymbol{z})^2 p(\boldsymbol{z})\mathrm{d}\boldsymbol{z}\mathrm{d}\boldsymbol{y}.$$

Then we have

$$\begin{aligned}\widetilde{\mathrm{SCE}}(\boldsymbol{Y}|\boldsymbol{Z}) - \widetilde{\mathrm{SCE}}(\boldsymbol{Y}|\boldsymbol{X}) &= \frac{1}{2}\iint p(\boldsymbol{y}|\boldsymbol{x})^2 p(\boldsymbol{x})\mathrm{d}\boldsymbol{y}\mathrm{d}\boldsymbol{x} - \frac{1}{2}\iint p(\boldsymbol{y}|\boldsymbol{z})^2 p(\boldsymbol{z})\mathrm{d}\boldsymbol{z}\mathrm{d}\boldsymbol{y} \\ &= \frac{1}{2}\iint p(\boldsymbol{y}|\boldsymbol{x})^2 p(\boldsymbol{x})\mathrm{d}\boldsymbol{x}\mathrm{d}\boldsymbol{y} + \frac{1}{2}\iint p(\boldsymbol{y}|\boldsymbol{z})^2 p(\boldsymbol{z})\mathrm{d}\boldsymbol{z}\mathrm{d}\boldsymbol{y} \\ &\quad - \iint p(\boldsymbol{y}|\boldsymbol{z})^2 p(\boldsymbol{z})\mathrm{d}\boldsymbol{z}\mathrm{d}\boldsymbol{y}.\end{aligned}$$

Let $p(\boldsymbol{x}) = p(\boldsymbol{z}, \boldsymbol{z}_\perp)$, and $\mathrm{d}\boldsymbol{x} = \mathrm{d}\boldsymbol{z}\mathrm{d}\boldsymbol{z}_\perp$. Then the final term can be expressed as

$$\begin{aligned}\iint p(\boldsymbol{y}|\boldsymbol{z})^2 p(\boldsymbol{z})\mathrm{d}\boldsymbol{z}\mathrm{d}\boldsymbol{y} &= \iint \frac{p(\boldsymbol{z},\boldsymbol{y})}{p(\boldsymbol{z})}\frac{p(\boldsymbol{z},\boldsymbol{y})}{p(\boldsymbol{z})}p(\boldsymbol{z})\mathrm{d}\boldsymbol{z}\mathrm{d}\boldsymbol{y} \\ &= \iint \frac{p(\boldsymbol{z},\boldsymbol{y})}{p(\boldsymbol{z})}p(\boldsymbol{z},\boldsymbol{y})\mathrm{d}\boldsymbol{z}\mathrm{d}\boldsymbol{y} \\ &= \iint \frac{p(\boldsymbol{z},\boldsymbol{y})}{p(\boldsymbol{z})}p(\boldsymbol{z}_\perp|\boldsymbol{z},\boldsymbol{y})p(\boldsymbol{z},\boldsymbol{y})\mathrm{d}\boldsymbol{z}\mathrm{d}\boldsymbol{z}_\perp\mathrm{d}\boldsymbol{y} \\ &= \iint \frac{p(\boldsymbol{z},\boldsymbol{y})}{p(\boldsymbol{z})}p(\boldsymbol{z},\boldsymbol{z}_\perp,\boldsymbol{y})\mathrm{d}\boldsymbol{z}\mathrm{d}\boldsymbol{z}_\perp\mathrm{d}\boldsymbol{y} \\ &= \iint \frac{p(\boldsymbol{z},\boldsymbol{y})}{p(\boldsymbol{z})}p(\boldsymbol{x},\boldsymbol{y})\mathrm{d}\boldsymbol{x}\mathrm{d}\boldsymbol{y} \\ &= \iint \frac{p(\boldsymbol{z},\boldsymbol{y})}{p(\boldsymbol{z})}\frac{p(\boldsymbol{x},\boldsymbol{y})}{p(\boldsymbol{x})}p(\boldsymbol{x})\mathrm{d}\boldsymbol{x}\mathrm{d}\boldsymbol{y} \\ &= \iint p(\boldsymbol{y}|\boldsymbol{z})p(\boldsymbol{y}|\boldsymbol{x})p(\boldsymbol{x})\mathrm{d}\boldsymbol{x}\mathrm{d}\boldsymbol{y},\end{aligned}$$

where $p(\boldsymbol{z}, \boldsymbol{z}_\perp, \boldsymbol{y}) = p(\boldsymbol{x}, \boldsymbol{y})$, and $\mathrm{d}\boldsymbol{z}\mathrm{d}\boldsymbol{z}_\perp = \mathrm{d}\boldsymbol{x}$ are used. Therefore,

$$\begin{aligned}
\widetilde{\mathrm{SCE}}(\boldsymbol{Y}|\boldsymbol{Z}) - \widetilde{\mathrm{SCE}}(Y|X) &= \frac{1}{2}\iint p(\boldsymbol{y}|\boldsymbol{x})^2 p(\boldsymbol{x})\mathrm{d}\boldsymbol{x}\mathrm{d}\boldsymbol{y} + \frac{1}{2}\iint p(\boldsymbol{y}|\boldsymbol{z})^2 p(\boldsymbol{z})\mathrm{d}\boldsymbol{z}\mathrm{d}\boldsymbol{y} \\
&\quad - \iint p(\boldsymbol{y}|\boldsymbol{z})p(\boldsymbol{y}|\boldsymbol{x})p(\boldsymbol{x})\mathrm{d}\boldsymbol{x}\mathrm{d}\boldsymbol{y} \\
&= \frac{1}{2}\iint \left(p(\boldsymbol{y}|\boldsymbol{x}) - p(\boldsymbol{y}|\boldsymbol{z})\right)^2 p(\boldsymbol{x})\mathrm{d}\boldsymbol{x}\mathrm{d}\boldsymbol{y}
\end{aligned}$$

We can also express $p(\boldsymbol{y}|\boldsymbol{x})$ in term of $p(\boldsymbol{y}|\boldsymbol{z})$ as

$$\begin{aligned}
p(\boldsymbol{y}|\boldsymbol{x}) &= \frac{p(\boldsymbol{x}, \boldsymbol{y})}{p(\boldsymbol{x})} \\
&= \frac{p(\boldsymbol{x}, \boldsymbol{y})}{p(\boldsymbol{x})}\frac{p(\boldsymbol{z}, \boldsymbol{y})}{p(\boldsymbol{z}, \boldsymbol{y})} \\
&= \frac{p(\boldsymbol{x}, \boldsymbol{y})p(\boldsymbol{z}, \boldsymbol{y})}{p(\boldsymbol{z}_\perp|\boldsymbol{z})p(\boldsymbol{z})p(\boldsymbol{y}|\boldsymbol{z})p(\boldsymbol{z})} \\
&= \frac{p(\boldsymbol{z}, \boldsymbol{z}_\perp, \boldsymbol{y})p(\boldsymbol{z}, \boldsymbol{y})}{p(\boldsymbol{z}_\perp|\boldsymbol{z})p(\boldsymbol{z})p(\boldsymbol{y}|\boldsymbol{z})p(\boldsymbol{z})} \\
&= \frac{p(\boldsymbol{z}_\perp, \boldsymbol{y}|\boldsymbol{z})p(\boldsymbol{z}, \boldsymbol{y})}{p(\boldsymbol{z}_\perp|\boldsymbol{z})p(\boldsymbol{y}|\boldsymbol{z})p(\boldsymbol{z})} \\
&= \frac{p(\boldsymbol{z}_\perp, \boldsymbol{y}|\boldsymbol{z})}{p(\boldsymbol{z}_\perp|\boldsymbol{z})p(\boldsymbol{y}|\boldsymbol{z})}p(\boldsymbol{y}|\boldsymbol{z})
\end{aligned}$$

Finally, we obtain

$$\begin{aligned}
\widetilde{\mathrm{SCE}}(\boldsymbol{Y}|\boldsymbol{Z}) - \widetilde{\mathrm{SCE}}(\boldsymbol{Y}|\boldsymbol{X}) &= \frac{1}{2}\iint \left(p(\boldsymbol{y}|\boldsymbol{x}) - p(\boldsymbol{y}|\boldsymbol{z})\right)^2 p(\boldsymbol{x})\mathrm{d}\boldsymbol{x}\mathrm{d}\boldsymbol{y} \\
&= \frac{1}{2}\iint \left(\frac{p(\boldsymbol{z}_\perp, \boldsymbol{y}|\boldsymbol{z})}{p(\boldsymbol{z}_\perp|\boldsymbol{z})p(\boldsymbol{y}|\boldsymbol{z})}p(\boldsymbol{y}|\boldsymbol{z}) - p(\boldsymbol{y}|\boldsymbol{z})\right)^2 p(\boldsymbol{x})\mathrm{d}\boldsymbol{x}\mathrm{d}\boldsymbol{y} \\
&= \frac{1}{2}\iint \left(\frac{p(\boldsymbol{z}_\perp, \boldsymbol{y}|\boldsymbol{z})}{p(\boldsymbol{z}_\perp|\boldsymbol{z})p(\boldsymbol{y}|\boldsymbol{z})} - 1\right)^2 p(\boldsymbol{y}|\boldsymbol{z})^2 p(\boldsymbol{x})\mathrm{d}\boldsymbol{x}\mathrm{d}\boldsymbol{y} \\
&\geq 0,
\end{aligned}$$

which concludes the proof.

B Derivatives of SCE

Here we show the formula of derivatives of $\widehat{\mathrm{SCE}}(Y|Z)$ using LSCE estimator. SCE approximation by LSCE estimator is

$$\widehat{\mathrm{SCE}}(\boldsymbol{Y}|\boldsymbol{Z}) = \frac{1}{2}\widehat{\boldsymbol{\alpha}}^\top \widehat{\boldsymbol{G}}\widehat{\boldsymbol{\alpha}} - \widehat{\boldsymbol{h}}^\top \widehat{\boldsymbol{\alpha}}.$$

Taking its partial derivatives with respect to $\boldsymbol{W}$ and we obtain

$$\begin{aligned}
\frac{\partial \widehat{\mathrm{SCE}}}{\partial W_{l,l'}} &= -\frac{1}{2}\frac{\partial \widehat{\boldsymbol{\alpha}}^\top \widehat{\boldsymbol{G}}\widehat{\boldsymbol{\alpha}}}{\partial W_{l,l'}} - \frac{\partial \widehat{\boldsymbol{h}}^\top \widehat{\boldsymbol{\alpha}}}{\partial W_{l,l'}} \\
&= \frac{1}{2}\left(\frac{\partial \widehat{\boldsymbol{\alpha}}^\top}{\partial W_{l,l'}}\widehat{\boldsymbol{G}}\widehat{\boldsymbol{\alpha}} + \frac{(\widehat{\boldsymbol{G}}\widehat{\boldsymbol{\alpha}})^\top}{\partial W_{l,l'}}\widehat{\boldsymbol{\alpha}}\right) - \frac{\partial \widehat{\boldsymbol{\alpha}}^\top}{\partial W_{l,l'}}\widehat{\boldsymbol{h}} - \frac{\partial \widehat{\boldsymbol{h}}^\top}{\partial W_{l,l'}}\widehat{\boldsymbol{\alpha}} \\
&= \frac{1}{2}\frac{\partial \widehat{\boldsymbol{\alpha}}^\top}{\partial W_{l,l'}}\widehat{\boldsymbol{G}}\widehat{\boldsymbol{\alpha}} + \frac{1}{2}\frac{\partial \widehat{\boldsymbol{\alpha}}^\top}{\partial W_{l,l'}}\widehat{\boldsymbol{G}}\widehat{\boldsymbol{\alpha}} + \frac{1}{2}\widehat{\boldsymbol{\alpha}}^\top\frac{\partial \widehat{\boldsymbol{G}}}{\partial W_{l,l'}}\widehat{\boldsymbol{\alpha}} - \frac{\partial \widehat{\boldsymbol{\alpha}}^\top}{\partial W_{l,l'}}\widehat{\boldsymbol{h}} - \frac{\partial \widehat{\boldsymbol{h}}^\top}{\partial W_{l,l'}}\widehat{\boldsymbol{\alpha}} \\
&= \frac{\partial \widehat{\boldsymbol{\alpha}}^\top}{\partial W_{l,l'}}\widehat{\boldsymbol{G}}\widehat{\boldsymbol{\alpha}} + \frac{1}{2}\widehat{\boldsymbol{\alpha}}^\top\frac{\partial \widehat{\boldsymbol{G}}}{\partial W_{l,l'}}\widehat{\boldsymbol{\alpha}} - \frac{\partial \widehat{\boldsymbol{\alpha}}^\top}{\partial W_{l,l'}}\widehat{\boldsymbol{h}} - \frac{\partial \widehat{\boldsymbol{h}}^\top}{\partial W_{l,l'}}\widehat{\boldsymbol{\alpha}}. \qquad (12)
\end{aligned}$$

Next we consider the partial derivatives of $\widehat{\boldsymbol{\alpha}}$ as follows

$$\begin{aligned}
\frac{\partial \widehat{\boldsymbol{\alpha}}}{\partial W_{l,l'}} &= \frac{\partial (\widehat{\boldsymbol{G}} + \lambda \boldsymbol{I})^{-1}\widehat{\boldsymbol{h}}}{\partial W_{l,l'}} \\
&= \frac{\partial (\widehat{\boldsymbol{G}} + \lambda \boldsymbol{I})^{-1}}{\partial W_{l,l'}}\widehat{\boldsymbol{h}} + (\widehat{\boldsymbol{G}} + \lambda \boldsymbol{I})^{-1}\frac{\partial \widehat{\boldsymbol{h}}}{\partial W_{l,l'}} \\
\frac{\partial \widehat{\boldsymbol{\alpha}}^\top}{\partial W_{l,l'}} &= (\frac{\partial (\widehat{\boldsymbol{G}} + \lambda \boldsymbol{I})^{-1}}{\partial W_{l,l'}}\widehat{\boldsymbol{h}})^\top + \frac{\partial \widehat{\boldsymbol{h}}^\top}{\partial W_{l,l'}}(\widehat{\boldsymbol{G}} + \lambda \boldsymbol{I})^{-1}. \qquad (13)
\end{aligned}$$

Using $\frac{\partial \boldsymbol{X}^{-1}}{\partial t} = -\boldsymbol{X}^{-1}\frac{\partial \boldsymbol{X}}{\partial t}\boldsymbol{X}^{-1}$, we obtain

$$\begin{aligned}
\frac{\partial (\widehat{\boldsymbol{G}} + \lambda \boldsymbol{I})^{-1}}{\partial W_{l,l'}}\widehat{\boldsymbol{h}} &= -(\widehat{\boldsymbol{G}} + \lambda \boldsymbol{I})^{-1}\frac{\partial \widehat{\boldsymbol{G}}}{\partial W_{l,l'}}(\widehat{\boldsymbol{G}} + \lambda \boldsymbol{I})^{-1}\widehat{\boldsymbol{h}} - (\widehat{\boldsymbol{G}} + \lambda \boldsymbol{I})^{-1}\frac{\partial \lambda \boldsymbol{I}}{\partial W_{l,l'}}(\widehat{\boldsymbol{G}} + \lambda \boldsymbol{I})^{-1}\widehat{\boldsymbol{h}} \\
&= -(\widehat{\boldsymbol{G}} + \lambda \boldsymbol{I})^{-1}\frac{\partial \widehat{\boldsymbol{G}}}{\partial W_{l,l'}}\widehat{\boldsymbol{\alpha}} - 0 \\
(\frac{\partial (\widehat{\boldsymbol{G}} + \lambda \boldsymbol{I})^{-1}}{\partial W_{l,l'}}\widehat{\boldsymbol{h}})^\top &= -\widehat{\boldsymbol{\alpha}}^\top\frac{\partial \widehat{\boldsymbol{G}}}{\partial W_{l,l'}}(\widehat{\boldsymbol{G}} + \lambda \boldsymbol{I})^{-1}. \qquad (14)
\end{aligned}$$

Substitute Eq.(14) into Eq.(13) to obtain

$$\frac{\partial \widehat{\boldsymbol{\alpha}}^\top}{\partial W_{l,l'}} = -\widehat{\boldsymbol{\alpha}}^\top\frac{\partial \widehat{\boldsymbol{G}}}{\partial W_{l,l'}}(\widehat{\boldsymbol{G}} + \lambda \boldsymbol{I})^{-1} + \frac{\partial \widehat{\boldsymbol{h}}^\top}{\partial W_{l,l'}}(\widehat{\boldsymbol{G}} + \lambda \boldsymbol{I})^{-1}. \qquad (15)$$

Finally, by substitute Eq.(15) into Eq.(12) and use $(\widehat{\boldsymbol{G}} + \lambda \boldsymbol{I})^{-1}\widehat{\boldsymbol{G}}\widehat{\boldsymbol{\alpha}} = \widehat{\boldsymbol{\beta}}$, we have

$$\begin{aligned}
\frac{\partial \widehat{\mathrm{SCE}}}{\partial W_{l,l'}} &= -\widehat{\boldsymbol{\alpha}}^\top\frac{\partial \widehat{\boldsymbol{G}}}{\partial W_{l,l'}}\widehat{\boldsymbol{\beta}} + \frac{\partial \widehat{\boldsymbol{h}}^\top}{\partial W_{l,l'}}\widehat{\boldsymbol{\beta}} + \frac{1}{2}\widehat{\boldsymbol{\alpha}}^\top\frac{\partial \widehat{\boldsymbol{G}}}{\partial W_{l,l'}}\widehat{\boldsymbol{\alpha}} \\
&\quad + \widehat{\boldsymbol{\alpha}}^\top\frac{\partial \widehat{\boldsymbol{G}}}{\partial W_{l,l'}}\widehat{\boldsymbol{\alpha}} - \frac{\partial \widehat{\boldsymbol{h}}^\top}{\partial W_{l,l'}}\widehat{\boldsymbol{\alpha}} - \frac{\partial \widehat{\boldsymbol{h}}^\top}{\partial W_{l,l'}}\widehat{\boldsymbol{\alpha}} \\
&= \widehat{\boldsymbol{\alpha}}^\top\frac{\partial \widehat{\boldsymbol{G}}}{\partial W_{l,l'}}(\frac{3}{2}\widehat{\boldsymbol{\alpha}} - \widehat{\boldsymbol{\beta}}) + \frac{\partial \widehat{\boldsymbol{h}}^\top}{\partial W_{l,l'}}(\widehat{\boldsymbol{\beta}} - 2\widehat{\boldsymbol{\alpha}}),
\end{aligned}$$

where the partial derivatives of $\widehat{\boldsymbol{G}}$ and $\widehat{\boldsymbol{h}}$ depend on the choice of basis function.

Here we consider the Gaussian basis function described in Section 2.4. Their partial derivatives are given by

$$\frac{\partial \widehat{G}_{k,k'}}{\partial W_{l,l'}} = -\frac{1}{\sigma^2 n} \sum_{i=1}^{n} \bar{\Phi}_{k,k'}(\boldsymbol{z}_i) \left((\boldsymbol{z}_i^{(l)} - \boldsymbol{u}_k^{(l)})(\boldsymbol{x}_i^{(l')} - \tilde{\boldsymbol{u}}_k^{(l')}) + (\boldsymbol{z}_i^{(l)} - \boldsymbol{u}_{k'}^{(l)})(\boldsymbol{x}_i^{(l')} - \tilde{\boldsymbol{u}}_{k'}^{(l')}) \right)$$

$$\frac{\partial \widehat{h}_k}{\partial W_{l,l'}} = -\frac{1}{\sigma^2 n} \sum_{i=1}^{n} \varphi_k(\boldsymbol{z}_i, \boldsymbol{y}_i) \left((\boldsymbol{z}_i^{(l)} - \boldsymbol{u}_k^{(l)})(\boldsymbol{x}_i^{(l')} - \tilde{\boldsymbol{u}}_k^{(l')}) \right).$$